

Supplementary Materials and Methods

Cell Culture and materials

Hep3B and HepG2 cell lines were grown in DMEM high glucose supplemented with 10% FBS and 50 mg/ml of a Pen/Strep mix in a 37°C/5% CO₂ humidified incubator. Mevalonate and lanosterol were from Sigma-Aldrich (St. Louis, MO). The primary antibodies used include those against TM6SF2 (sc-169600), GAPDH (sc-25778), ABCG5 (sc-25796) and ABCG8 (sc-30111) from Santa Cruz Biotechnology (Dallas, Texas). ER stress antibody sampler kit (#9956) from Cell Signaling Technology (Danvers, MA). Purified anti-XBP-1 (619501) was from BioLegend (San Diego, CA).

Protein Extraction and Western Blotting

Tissue extracts were prepared with tissue extraction reagents (Thermo Fisher Scientific, Grand Island, NY). Protein extracts were resolved by SDS-PAGE using 10% gels and electro blotted onto PVDF membranes (Bio-Rad). Membranes were blocked for 1 h at room temperature in TBS Tween 20 containing 5% (w/v) nonfat dry milk powder, and incubated overnight with primary antibodies diluted 1:500–1000 in 5% nonfat milk solution. After washing, membranes were incubated with IRDye-conjugated IgG (LI-COR Biosciences, Lincoln, NE) secondary antibody diluted 1:5000 for 1 h. After washing with TBST, blots were scanned, and the image was displayed in grayscale. The intensity of the protein band was quantified using an image processing program (Li-Cor Odyssey).

Quantitative Real-Time Reverse Transcription Polymerase Chain Reaction

Total RNA from mouse liver samples was extracted using TRIzol® reagent (Invitrogen, Grand Island, NY) according to the manufacturer's instructions. Total RNA from cultured mammalian cells was extracted using the RNeasy kit (Qiagen, Valencia, CA). RNA was reverse-transcribed into cDNA with SuperScript III and random primers (Invitrogen). Specific transcript levels were assessed by a real-time PCR system (Bio-Rad, Hercules, CA) using iQ SYBR Green Supermix (Bio-Rad). Unless indicated otherwise, the relative quantification for each gene of interest was normalized against the internal control, Gapdh. The primers used in this study are listed in Supplementary Table 1.

Histology

Liver slides were stained with Picrosirius Red (PSR) stain kit (PolyScience, #24901, Warrington, PA) according to the manufacturer's instructions. Computer-assisted quantification of liver fibrosis in PSR stained sections was performed using a customized Image J macro. The mouse tissues were routinely counter stained with haematoxylin and eosin (H&E) staining as described previously.¹ Inflammation status was evaluated in the H&E-stained sections. For inflammation score, 0 was defined as no inflammatory foci, 1 was defined as <2 foci per 200 x field, 2 was defined as 2-4 foci per 200 x field, 3 was defined as >4 foci per 200 x field.^{2,3}

Oil Red O (ORO) Staining

Mouse livers were fixed with 4% paraformaldehyde and then impregnated with 30% sucrose until they sank. Frozen liver sections (8 μm) were stained with 5% Oil Red O (Sigma-Aldrich, St. Louis, MO) for 15 min and then stained with haematoxylin. Sections were then examined under light microscopy. A total of 6 tissue sections were analyzed for each animal.

Detection of Total Cholesterol (TC)

TC in the liver was determined with a TC assay kit (Cell Biolabs, STA-384, San Diego, CA) following the manufacturer's recommendation. In brief, the liver cholesterol was extracted with a mixture of chloroform: isopropanol: NP-40 (7:11:0.1) in a micro-homogenizer. Each cholesterol standard and sample was assayed in duplicate or triplicate. After the cholesterol reaction was completed, the plate was read with a spectrophotometric microplate reader in the 540-570 nm range. The concentration of cholesterol was calculated by comparing the sample absorbance values to the standard curve and normalized to the liver sample weight.

Intracellular Cholesterol Detection

The intracellular cholesterol in HepG2 cells was detected based on the intensity of Filipin III fluorescence with a kit from Cayman Chemical Company (10009779) according to the manufacturer's instructions.

Detection of liver Triglyceride (TG)

TG in the liver was determined with a TG assay kit (BioVision, K622-100, Milpitas, CA) following the manufacturer's recommendation. In brief, the liver TG was extracted with solution containing 5% NP-40 in water. Each TG standard and sample was assayed in duplicate or triplicate. After the cholesterol reaction was completed, the plate was read with a spectrophotometric microplate reader at 570 nm. The concentration of TG was calculated by comparing the sample absorbance values to the standard curve and normalized to the liver sample weight.

Alanine Aminotransferase (ALT) and Aspartate Aminotransferase (AST) Activity Assay

The ALT and AST enzyme activity in mouse serum was determined with an ALT assay kit (Sigma-Aldrich, MAK052) and AST assay kit (Sigma-Aldrich, MAK055, St. Louis, MO), respectively, according to the manufacturer's instructions.

References:

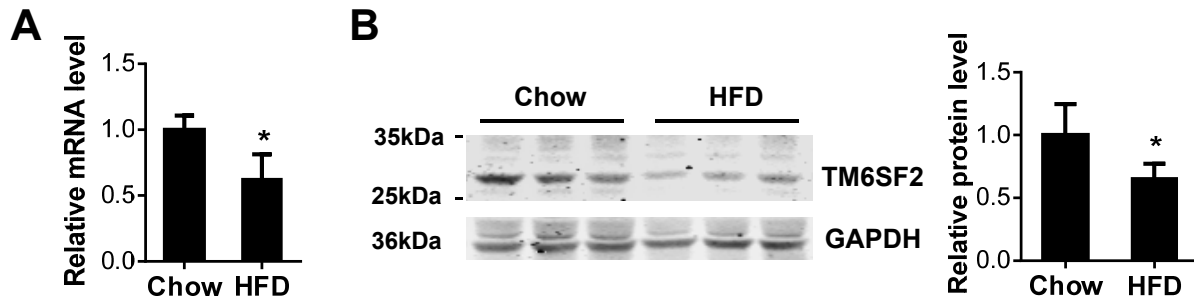
1. Chang L, Villacorta L, Li R, et al. Loss of perivascular adipose tissue on peroxisome proliferator-activated receptor-gamma deletion in smooth muscle cells impairs intravascular thermoregulation and enhances atherosclerosis. *Circulation* 2012;126:1067-78.
2. Brunt EM, Tiniakos DG. Histopathology of nonalcoholic fatty liver disease. *World J Gastroenterol* 2010;16:5286-96.
3. Kleiner DE, Brunt EM, Van Natta M, et al. Design and validation of a histological scoring system for nonalcoholic fatty liver disease. *Hepatology* 2005;41:1313-21.

Supplementary Table 1

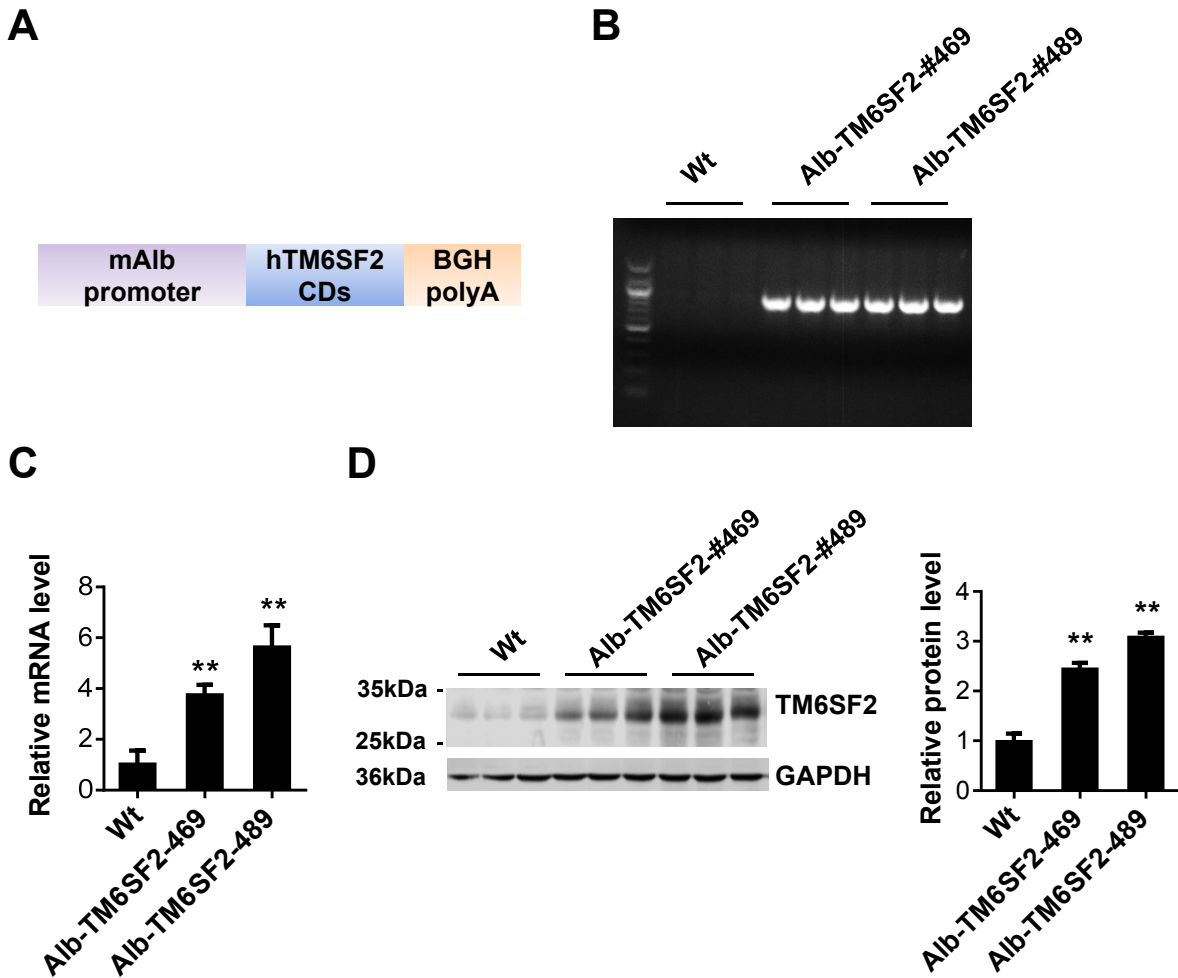
Primers for Real-time PCR and Genotyping

Gene*	Forward (5'-3')	Reverse (5'-3')
mTm6sf2	caagtttcggcgttctcaca	tgaagcccatcatgtagcca
mCd36,	gaatgggctgtgatcggaac	acgtcatctgggtttgcac
mCyp7a1	cacttggtcaagaccgcaca	gtgtttgcttgagatgcca
mCyp8b1	gtacgcttctctatcgct	ctggagggatggcgtcttat
mCyp2c54	atggggatgtctttgctgga	tcctctgaacacggctctc
mCyp27a1	cttcatcgcaacaaggagagc	ccaaggcaaggtagtagaga
mAbcg5	cagtatagtgccctgctca	ccacaagtgaagttcaggcc
mAbcg8	cacctccacatgctctct	ttcaggccatggcactgat
mGapdh	ctggactcaacagcaact	gagttgggataggcctctc
mMcp-1	aggtccctgtcatgctctg	tctggaccattccttctg
mAcat2-1	ccaccacctggacagtct	agccctgatgactgattgg
mDhcr7-1	cgctcccaaagtcaagagtc	gtgtcttgcccaaagtct
mDhcr24-1	cactcagctgctatgggaca	agggattcatgccttctct
mHmgcr-1	tggagatcatgtgctgcttc	gcgactatgagcgtgaacaa
mHmgcs1-1	tttgatgcagctgtttgagg	ccacctgtaggtctggcatt
mLss-1	gctgcatgtggtgatggac	gagaaacgtgctcctggaag
mPmvk-1	gaagattgtggaaggcgtgt	tctgactcagcatcgccac
mSc5d-1	atgcttttcaccctgtggac	gtgggtgctgtgtggtgag
TM6SF2 transgene	ttctacaccaaggagggtgagc	aacaccaggatgctcatggcga
Alb-TM6SF2 genotyping	gaaccaatgaaatgcgaggt	agaagccagcaaggatgaga
Tm6sf2 KO genotyping	ctgaaaactgggaaaggacgct	tggagagggatttctgcttga

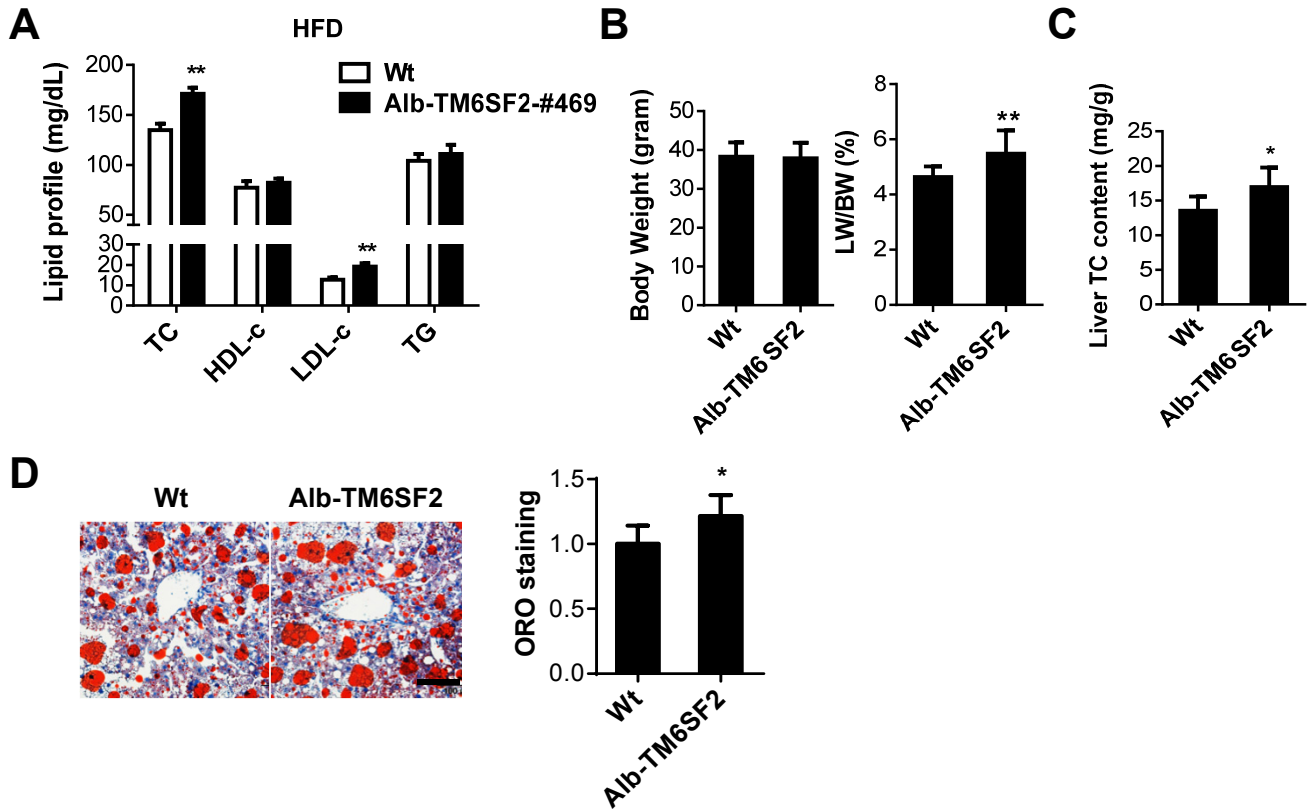
* “m” denotes mouse.



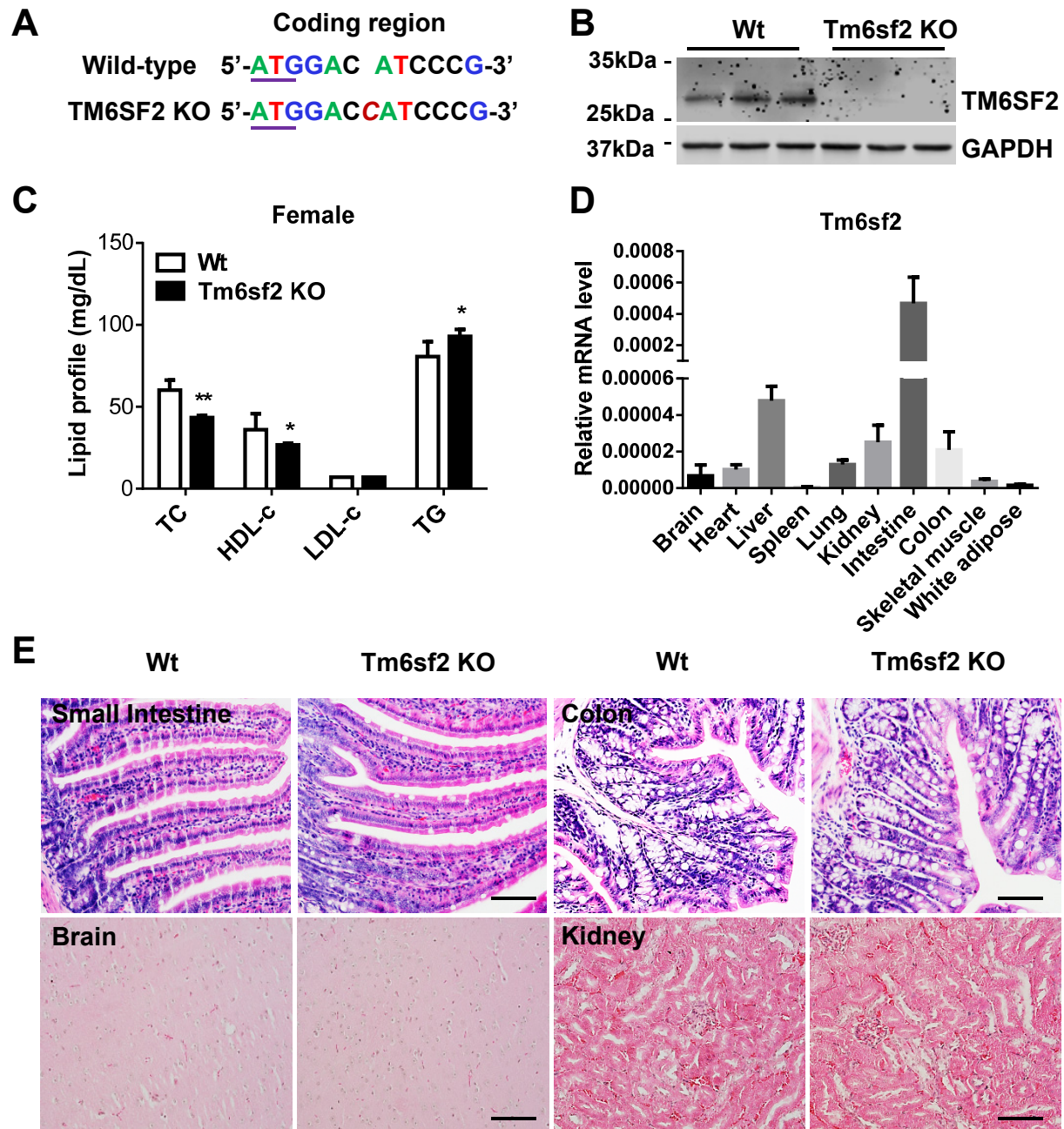
Supplementary Figure 1. TM6SF2 is downregulated in livers of HFD-fed mice. (A), C57BL/6 mice were fed a chow diet or high fat diet (HFD) for 10 weeks, and the expression of TM6SF2 in livers was determined by Real-time PCR, n = 5 per group. (B), The expression of TM6SF2 was determined by Western blot. The band intensity was quantitatively analyzed and normalized to GAPDH. Values are mean \pm SD. *, $P < .05$.



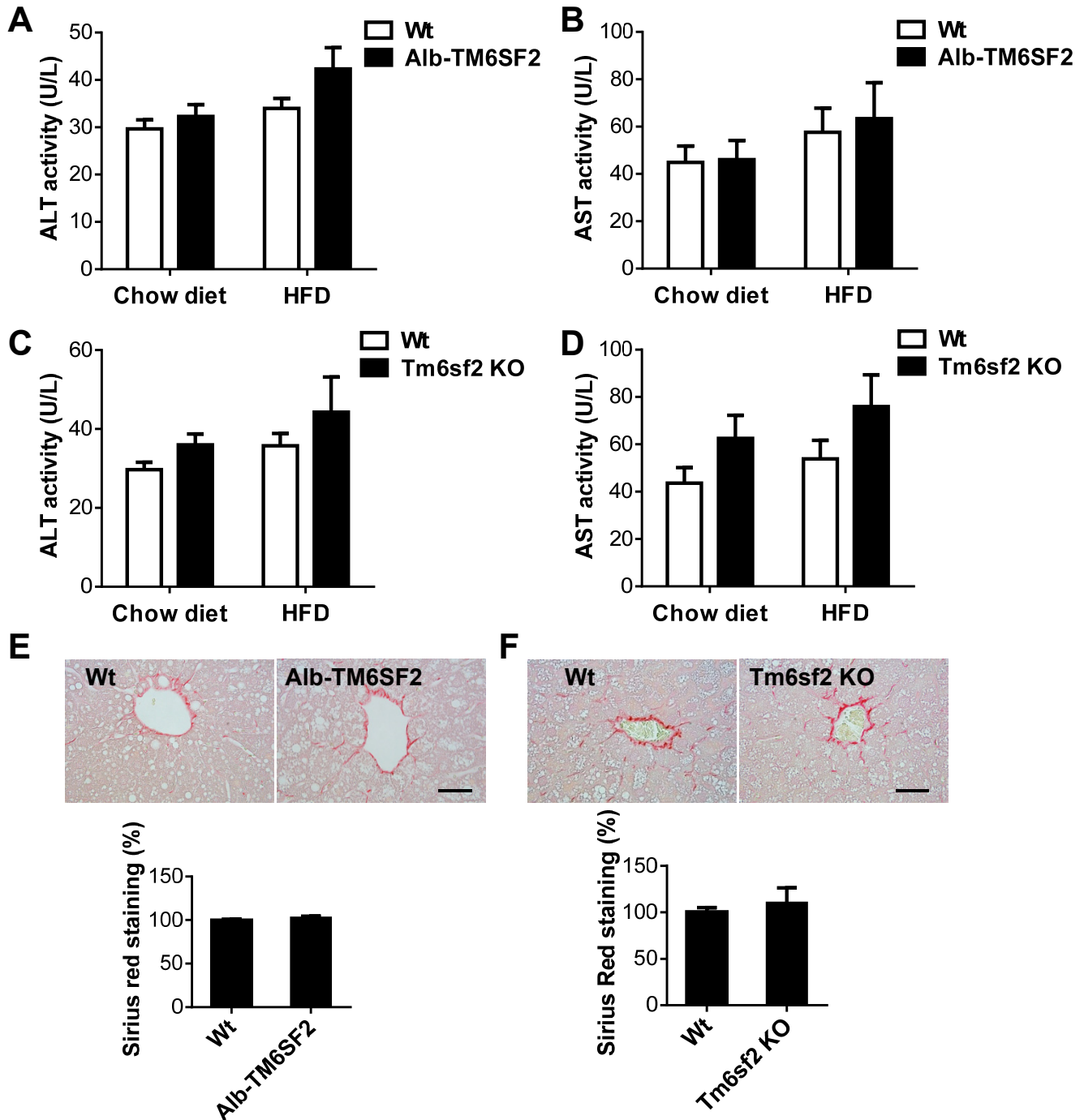
Supplementary Figure 2. Genotyping of TM6SF2 transgenic mice. (A), Schema for the generation of mouse albumin (mAlb) promoter-driven human TM6SF2 transgenic mice. (B), Genotyping of Alb-TM6SF2 transgenic mice. (C), The expression of TM6SF2 in livers of the wild type (Wt) and Alb-TM6SF2 transgenic mice was determined by Real-time PCR (n = 4-5 per group). (D), The expression of TM6SF2 was detected by Western blot and the band intensity was quantitatively analyzed and normalized to GAPDH. Values are mean \pm SD. *, $P < .05$; **, $P < .01$.



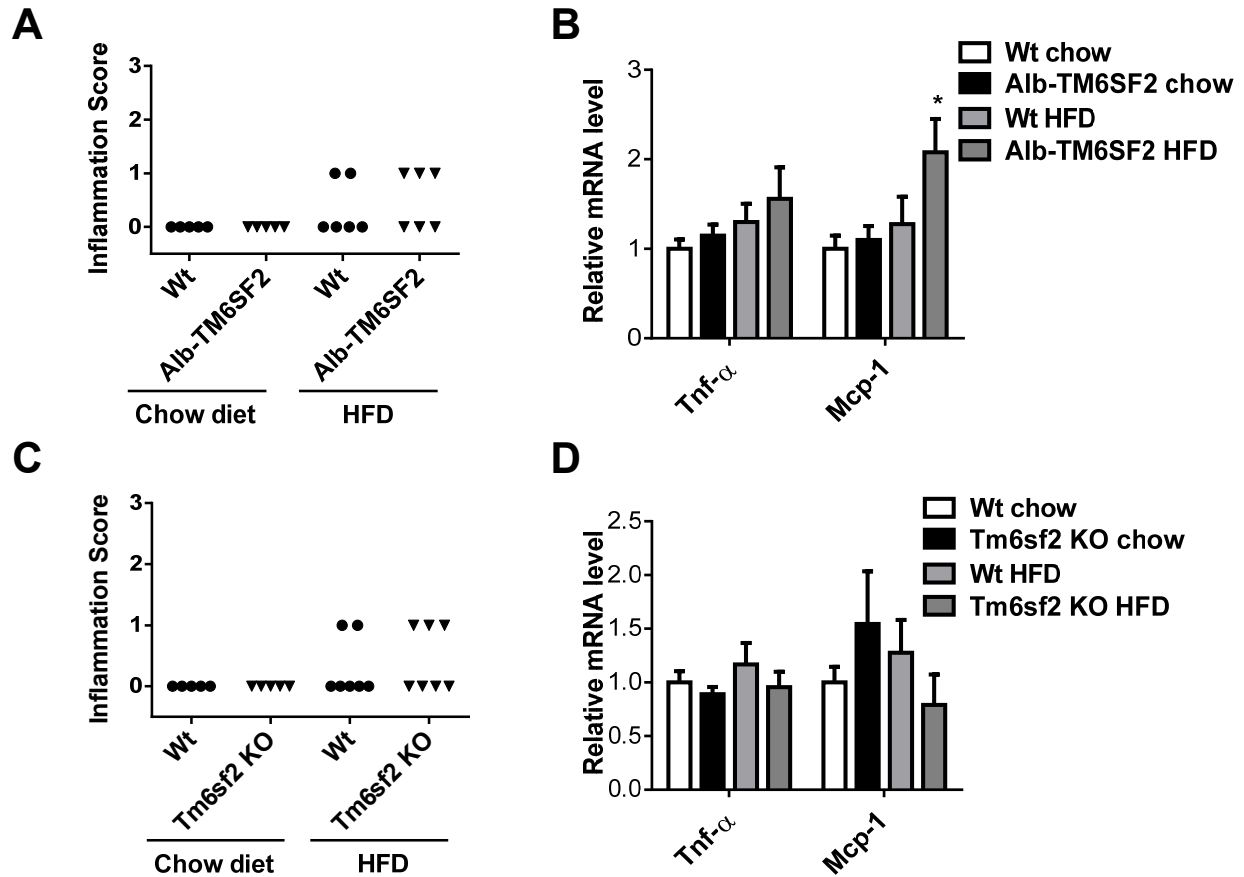
Supplementary Figure 3. Lipid profile in Alb-TM6SF2 transgenic mice. A second line (#469) of Alb-TM6SF2 transgenic mice fed a HFD for 10 weeks. (A), Lipid profile was measured enzymatically. (B), The BW and LW/BW was determined. (C), TC in the liver was extracted and detected. (D), Sections from the liver tissue of the same mice were stained with ORO and quantitatively analyzed. Scale bar=100 μ m. N= 7-8 per group. Values are mean \pm SD. *, $P < .05$; **, $P < .01$.



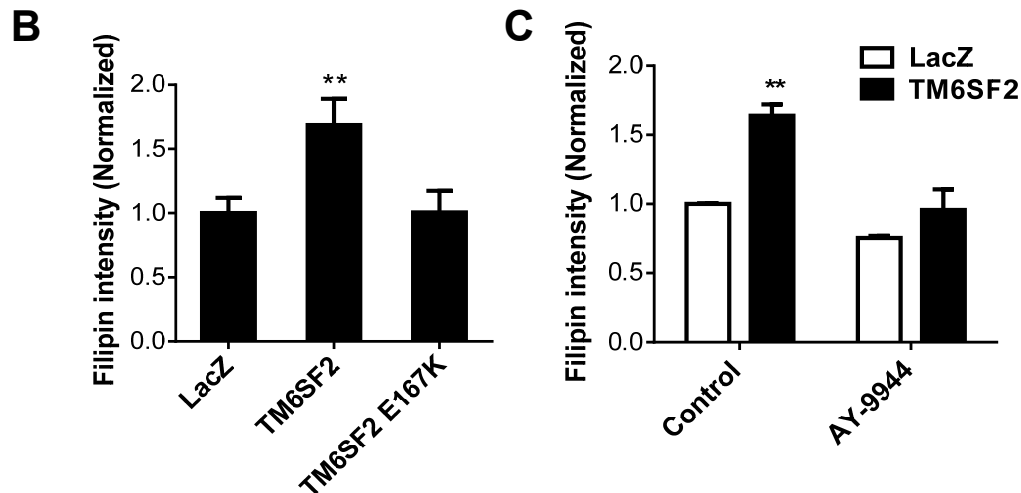
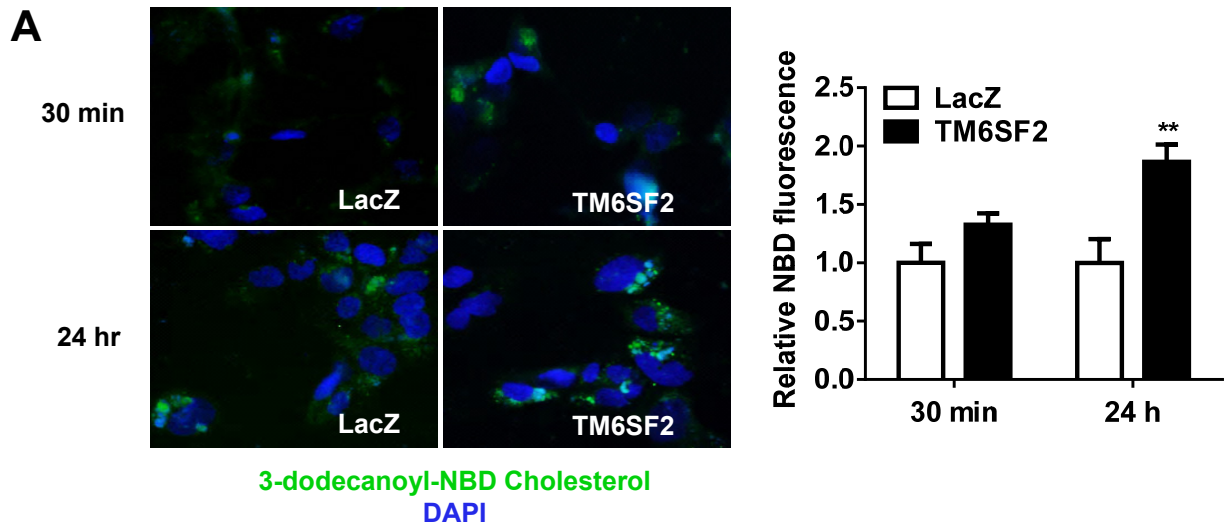
Supplementary Figure 4. Characterization of Tm6sf2 KO mice fed a chow diet. (A), Generation of Tm6sf2 KO mice by CRISPR/Cas9 technology. (B), The Tm6sf2 KO was confirmed by Western blot. (C), Eight-week-old female Tm6sf2 KO mice and control mice were fed a chow diet ($n = 8$ per group). The plasma levels of cholesterol and TG in the mice were determined enzymatically. Values are mean \pm SD. *, $P < .05$; **, $P < .01$. (D), Tissue distribution of Tm6sf2 in mouse was determined by Real-time PCR with 18S as the internal control. (E), Histological analysis of tissues from male Tm6sf2 KO mice and wild-type mice fed a chow diet by H&E staining. Scale bar= 100 μ m.



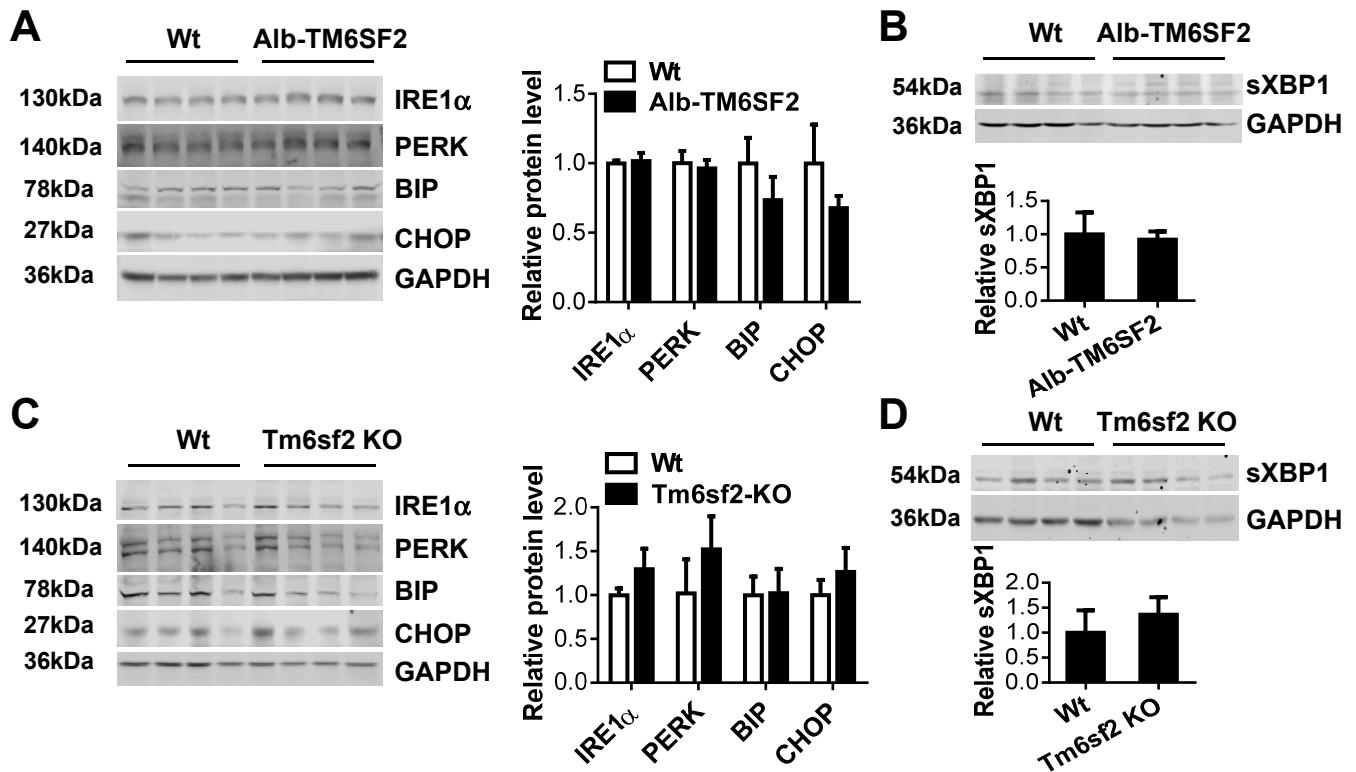
Supplementary Figure 5. Fibrosis in Tm6sf2 genetically engineered mice. (A-B), Eight-week-old Alb-TM6SF2-#489 and control mice were fed a chow diet or HFD for 10 weeks ($n = 5-7$ per group). The plasma ALT (A) and AST activity (B) were determined enzymatically in the mice. (C-D), Eight-week-old Tm6sf2 KO mice and control mice were fed a chow diet or HFD for 12 weeks ($n = 5-7$ per group). The plasma ALT (C) activity and AST activity (D) were determined enzymatically in the mice. Values in A-D are mean \pm SEM. (E), The liver fibrosis in Alb-TM6SF2 mice and control mice fed a HFD was measured by picosirius red staining and quantitatively analyzed. (F), The liver fibrosis in Tm6sf2 KO and control mice fed a HFD was measured by picosirius red staining and quantitatively analyzed ($n = 5-7$ per group). Values are mean \pm SD. Scale bar= 50 μ m in (E) and (F).



Supplementary Figure 6. The effect of TM6SF2 on inflammatory genes in the liver. (A-B), Eight-week-old Alb-TM6SF2-#489 and control mice were fed a chow diet or HFD for 10 weeks. (A), The inflammation score was assigned in a blinded fashion to H&E-stained samples for inflammation, N = 5-6. (B), The expression of Tnf- α and Mcp-1 was determined by Real-time PCR. (C-D), Eight-week-old Tm6sf2 KO and control mice were fed a chow diet or HFD for 12 weeks. (C), The inflammation score was assessed as described in B. N = 5-7. (D), The expression of Tnf- α and Mcp-1 was determined by Real-time PCR. Values are mean \pm SD. *, $P < .05$.



Supplementary Figure 7. The effect of TM6SF2 on cholesterol biosynthesis. (A), Hep3B cells were incubated with 3-dodecanoyl-NBD Cholesterol (15 $\mu\text{g}/\text{mL}$) in serum-free medium for 30 min, or 3-dodecanoyl-NBD Cholesterol (1.5 $\mu\text{g}/\text{mL}$) in serum-free medium for 24 h. The intracellular NBD-cholesterol was detected by immunofluorescence, and the fluorescence intensity was quantitatively analyzed by NIH ImageJ. Scale bar = 50 μm . (B), HepG2 cells were infected with Ad-TM6SF2, Ad-TM6SF2-E167K, or Ad-LacZ (20 MOI) and 48 h later, treated with hydroxypropyl- β -cyclodextrin (HPCD, 1% w/v) for 1 h, and then incubated with lanosterol (10 $\mu\text{mol}/\text{L}$) plus mevalonate (50 $\mu\text{mol}/\text{L}$) in 5% lipoprotein deficient serum (LPDS) DMEM for 24 h. (C), HepG2 cells were infected with Ad-TM6SF2 or Ad-LacZ (20 MOI) and 24 h later, pretreated with AY-9944 after cholesterol depletion by HPCD, and then incubated with lanosterol (10 $\mu\text{mol}/\text{L}$) in 5% LPDS DMEM for 24 h. The intracellular cholesterol was detected based on the intensity of Filipin III fluorescence. Values are mean \pm SD. **, $P < .01$.



Supplementary Figure 8. The effect of TM6SF2 on ER stress pathway. (A-B), Eight-week-old Alb-TM6SF2-#489 and control mice were fed a HFD for 10 weeks. The expression of ER stress proteins (A) and spliced XBP1 (sXBP1) (B) was determined by Western blot and quantitatively analyzed. (C-D), Eight-week-old Tm6sf2 KO mice and control mice were fed a HFD for 12 weeks. The expression of ER stress genes (C) and sXBP1 (D) was determined by Western blot and quantitatively analyzed. N= 4-5 per group. Values are mean \pm SD.